Random-matrix modeling of semilinear response, the generalized variable-range hopping picture, and the conductance of mesoscopic rings

Alexander Stotland,[1] Tsampikos Kottos,[2] and Doron Cohen[1]

[1]*Department of Physics, Ben-Gurion University, Beer-Sheva 84105, Israel*

[2]*Department of Physics, Wesleyan University, Middletown, Connecticut 06459, USA*

Semilinear response theory determines the absorption coefficient of a driven system using a resistor network calculation: each unperturbed energy level of a particle in a vibrating trap, or of an electron in a mesoscopic ring, is regarded as a node (n) of the network; the transition rates (w_{mn}) between the nodes are regarded as the elements of a random matrix that describes the network. If the size distribution of the connecting elements is wide (e.g., log-normal–like rather than Gaussian type) the result for the absorption coefficient differs enormously from the conventional Kubo prediction of linear response theory. We use a generalized variable range hopping scheme for the analysis. In particular, we apply this approach to obtain practical approximations for the conductance of mesoscopic rings. In this context Mott's picture of diffusion and localization is revisited.

I. INTRODUCTION

Semilinear response theory (SLRT) (Ref. [1–3]) provides a procedure for the calculation of the absorption coefficient of a driven system, assuming that there are well-defined transition rates w_{mn} between levels E_n that are ordered by energy. In this context it is helpful to regard w_{mn}^{-1} as describing resistors that connect nodes of a network, a point of view that has become popular in the related studies of variable range hopping (VRH).[4–9] In the random matrix theory (RMT) framework w_{mn} is a random matrix whose construction is inspired by analyzing the statistical properties of the Hamiltonian of an actual physical system.[10,11] Three physical applications have been discussed so far: (i) metallic rings driven by electromotive force;[12] (ii) metallic grains driven by low-frequency radiation;[3] and (iii) cold atoms that are heated up due to the vibrations of a wall.[13] It is crucial to observe that depending on the parameters that define the physical model, the matrix w_{mn} might be *banded* and *sparse*.[14,15] Consequently, nontrivial results that go beyond linear response theory (LRT) are obtained.

In order to have a precise mathematical definition of the RMT model, let us write the random matrix as

$$w_{mn} = X_{mn} \times \widetilde{B}(E_m - E_n). \tag{1}$$

In this expression $\widetilde{B}(\omega)$ describes the band profile of the matrix and X_{mn} is a random matrix whose entries x are positive uncorrelated random numbers. If $\log(x)$ is widely distributed over many decades, as in the case of log-normal or log-box distribution, then we say that the matrix is effectively sparse. Sparsity means that the majority of elements are very small compared with the average value.

Irrespective of real-space dimensionality, we regard the index n of the energy levels as labeling the nodes of a one-dimensional (1D) lattice (see Fig. 1) hence the w_{mn} define a 1D resistor network. The inverse resistivity of this network (see Appendix A) is denoted as $w = [[w_{mn}]]$ and has the meaning of diffusion coefficient. In proper units the relation is

$$D_{\mathrm{E}} = \varrho_{\mathrm{E}}^{-2} \times [[w_{mn}]], \tag{2}$$

$$\equiv G\varepsilon^2, \tag{3}$$

where ϱ_{E} is the mean density of states (DOS). The parameter ε represents the RMS amplitude of the driving field: it is the RMS displacement of a wall element if we consider the heating of cold atoms in a trap; it is the RMS voltage if we consider a ring that is driven by an electromotive-force (EMF). We assume here that $w_{mn} \propto \varepsilon^2$, which holds whenever the standard conditions of the Fermi-Golden rule (FGR) are satisfied.

Within the framework of the FGR picture the transitions rates w_{mn} are determined by the matrix elements V_{mn} of the perturbation term in the Hamiltonian. The naive expectation is to obtain the Kubo formula $G = \pi \varrho_{\mathrm{E}} \langle\langle |V_{mn}|^2 \rangle\rangle_{\mathrm{a}}$ for the absorption coefficient G. The calculation involves a weighted algebraic average
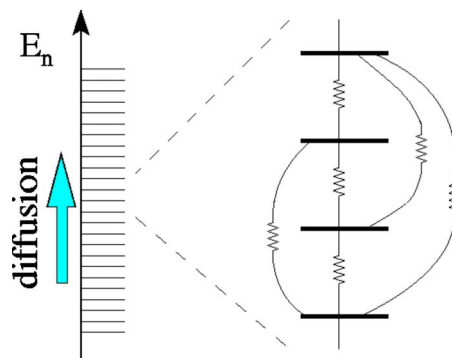

FIG. 1. (Color online) The driving induces transitions between levels E_n of a closed system, leading to diffusion in energy space and, hence, an associated heating. The diffusion coefficient D_{E} can be calculated using a resistor network analogy. Connected sequences of transitions are essential in order to have a nonvanishing result, as in the theory of percolation.

$$\langle\langle |V_{mn}|^2\rangle\rangle_{\mathrm{a}} = \int_{-\infty}^{\infty} \langle |V_{mn}|^2\rangle_\omega \widetilde{F}(\omega)\frac{d\omega}{2\pi}, \qquad (4)$$

where $\widetilde{F}(\omega)$ is a normalized function that describes the spectral content of the driving source and $\langle..\rangle_\omega$ is defined as the average value for $(E_m-E_n)\sim\omega$ transitions. A more careful inspection reveals that the Kubo calculation does not apply to the problem as defined above. In order to appreciate the difference we rewrite Eq. (2) as

$$G = \pi\varrho_{\mathrm{E}}\langle\langle |V_{mn}|^2\rangle\rangle. \qquad (5)$$

The double average notation indicates a *resistor-network* calculation. This SLRT "average" is bounded from above by the algebraic average of Eq. (4) and from below by the corresponding harmonic mean. Later in this paper we adopt a generalized VRH procedure in order to estimate the SLRT average

$$\langle\langle |V_{mn}|^2\rangle\rangle \approx \int_{-\infty}^{\infty} [|V_{mn}|^2]_\omega \widetilde{F}(\omega)\frac{d\omega}{2\pi}, \qquad (6)$$

where $[..]_\omega$ is the typical value for $(E_m-E_n)\sim\omega$ transitions. The notion of typical value will be defined later: it is determined by the size distribution of the matrix elements.

Physically the idea behind SLRT is very simple: in order to have "good" absorption it is essential to have *connected sequences* of transitions. Consequently, if w_{mn} is sparse, the traditional Kubo expression provides gross overestimate because it is based on an algebraic average calculation. Consequently, our interest is to calculate the *ratio* between the SLRT and the LRT conductance, which we define as the SLRT suppression factor

$$g_{\mathrm{SLRT}} \equiv \frac{\langle\langle |V_{mn}|^2\rangle\rangle}{\langle\langle |V_{mn}|^2\rangle\rangle_{\mathrm{a}}}, \qquad (7)$$

where $\langle\langle\ldots\rangle\rangle_{\mathrm{a}}$ denotes the usual weighted algebraic average that appears in the Kubo formula. Loosely speaking, if the percentage of *large* in-band elements is $s\ll1$ then a generalized VRH estimate might lead to a result of the type

$$g_{\mathrm{SLRT}} \sim \exp\left(-\frac{\mathrm{const}}{s^{\mathrm{power}}}\right). \qquad (8)$$

A few publications have been devoted to report various partial results that have been obtained using SLRT. The purpose of the present paper is to bridge between SLRT and the traditional literature, to further develop the analytical tools, and to provide elaborated tangible results that hopefully can be tested in actual experiments.

Our main focus concerns the Ohmic conductance G_{Ohm} of small metallic rings, which is related to the G of Eq. (5) via $G_{\mathrm{Ohm}}=\varrho_{\mathrm{E}}G$, where E is the Fermi energy. Up to a factor, the perturbation matrix consists of the elements v_{mn} of the velocity operator. Accordingly, G_{Ohm} is the LRT or the SLRT average over $|v_{mn}|^2$. Past literature has provided a theory for the conductance in the Debye or adiabatic regimes[16,17] where the FGR picture does not apply. Diffusive rings have been

further analyzed[18] in the Kubo regime and later weak-localization corrections have been incorporated[19,20] and verified experimentally.[21–23]

Still neither VRH in real space nor SLRT response in the ballistic regime had been considered in the context of mesoscopic conductance. In Fig. 2 we present some reprocessed numerical results that have been reported in Ref. 12. These numerical results indicate that indeed for both weak and strong disorder the matrix elements of the velocity operator become sparse with $s\ll1$. As explained in Ref. 12 this is related to the nonergodicity of the eigenstates. In the present paper we would like to present a full analysis of the conductance that starts from the strength of the disorder W as an input. The disorder determines the sparsity s, and then, using RMT modeling and a generalized VRH approximation, leads to some tangible results (Fig. 3) for the SLRT suppression factor g_{SLRT}. We also explain how this factor can be measured in an actual laboratory experiment and how *semilinear* response can be distinguished from *linear* response in a way that does not involve any ambiguities.

Outline. Section II motivates the study by introducing the physical model, including subsections that relate to the characterization of metallic rings and their Kubo-Drude conductance. Some more details are given in Appendices B and C. Section III discusses the RMT modeling in general. Section IV briefly reviews the SLRT calculation procedure. Section V elaborates on the generalized VRH approximation. Section VI introduces the analysis of some prototype non-Gaussian ensembles. Some more details are given in Appendices D and E. Section VII discusses the semiclassical theory of the matrix elements that are required for the calculation of the mesoscopic conductance. Section VIII discusses the SLRT calculation in the ballistic regime. Section IX discusses the SLRT calculation in the Anderson localization regime. Section X clarifies the relation between SLRT and the traditional VRH calculation. Section XI questions the possibility to get VRH from proper LRT analysis. Section XII contrasts VRH with nonthermal hopping due to noisy source. Section XIII proposes how to experimentally test SLRT via conductance measurements. Section XIV summarizes the major observations regarding the relation between SLRT, LRT, and VRH.

II. PHYSICAL MODEL

In order to physically motivate the analysis, we consider a particle of mass m in a rectangular box of length $L_x=L$ and width L_y. In one problem, that of Ref. 13, we had assumed Dirichlet boundary conditions and considered the response for vibrations of the wall. In the present paper we assume ring geometry with periodic boundary conditions on L_x and consider the response to EMF. In both cases the Hamiltonian matrix can be written as

$$\mathcal{H} = \mathrm{diag}\{E_n\} + \{U_{m,n}\} + f(t)\{V_{m,n}\}, \qquad (9)$$

where $\boldsymbol{n}=(n_x,n_y)$ labels the unperturbed eigenstates of a clean box/ring, $U(x,y)$ describes the potential floor (either smooth deformation or uncorrelated disorder), and V is the perturbation matrix due to the driving. Given that the energy of the particle is E we define $k_{\mathrm{E}}=(2\mathsf{m}E)^{1/2}$ and
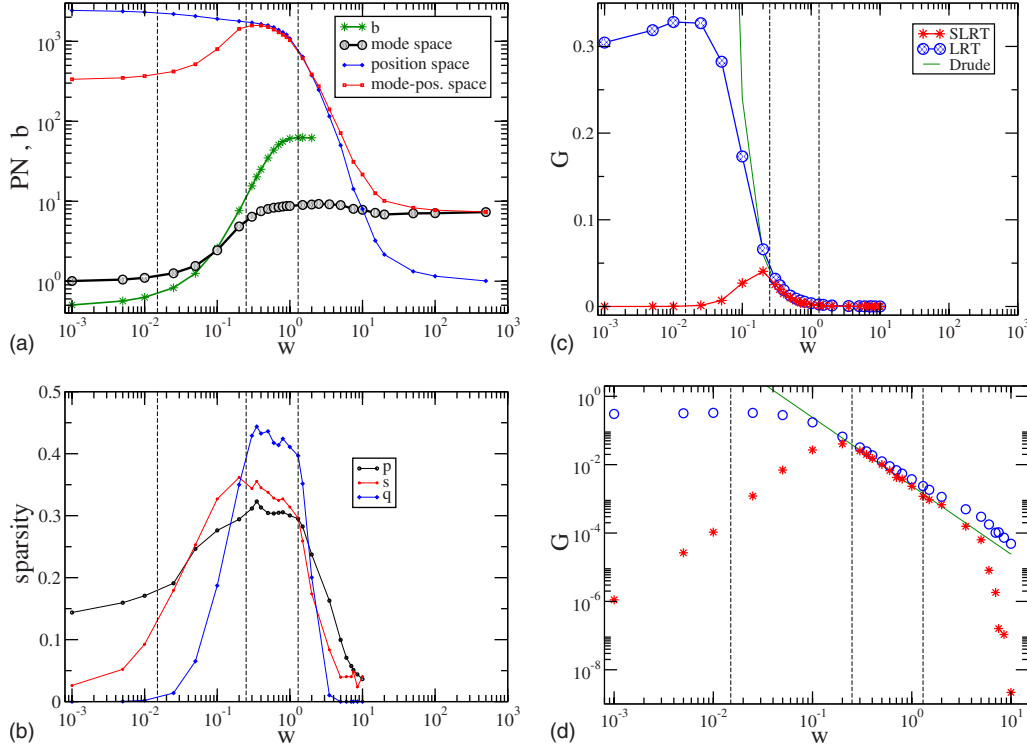
FIG. 2. (Color online) (a) The ergodicity of the eigenstates is characterized by the PN which is calculated in various representations (see Appendix B). The bandwidth b of v_{nm} constitutes another measure for mixing. The clean, ballistic, diffusive, and localization regimes (see Sec. II A) are separated by vertical lines. (b) The sparsity parameters (q, p, and s) that characterize the perturbation matrix v_{nm} are plotted versus the disorder W. (c) The scaled conductance in arbitrary units equals $\langle\langle|v_{mn}|^2\rangle\rangle$. The Drude, the LRT, and the SLRT results are displayed versus the strength of the disorder W. (d) The same plot in the logarithmic scale. We see that in the ballistic regime the SLRT conductance becomes worse as the disorder becomes weaker, in opposition with the Drude expectation.

$v_E = (2E/m)^{1/2}$. The associated number of open modes, i.e., the number of energetically allowed n_y values, is

$$\mathcal{M} = \frac{k_E L_y}{\pi}. \quad (10)$$

The density of states is

$$\varrho_E = \frac{m}{2\pi} L_x L_y = \mathcal{M} \frac{L}{2v_E}. \quad (11)$$

The static part of the Hamiltonian can be diagonalized and in the new basis the Hamiltonian takes the form

$$\mathcal{H} = \text{diag}\{E_n\} + f(t)\{V_{mn}\}, \quad (12)$$

where E_n are the perturbed energies. The power spectrum $\tilde{S}(\omega) = \varepsilon^2 \tilde{F}(\omega)$ of the low-frequency driving $\dot{f}$ is either rectangular with sharp cutoff at some frequency ω_c or exponential

$$\tilde{F}(\omega) = \frac{1}{2\omega_c} \exp\left(-\frac{|\omega|}{\omega_c}\right). \quad (13)$$

We assume that ω_c is small compared with any relevant semiclassical energy scale but larger compared with the mean-level spacing. If the driving is by a thermal source then ω_c can be identified as the *temperature* of the source. This

latter point of view is useful in the discussion of the relation between SLRT and VRH.

In the case of an EMF driven ring ε is the RMS of the voltage and the interaction $-f(t)V$ of the particle with the magnetic flux $f(t)$ involves $V = -(e/L)v$, where v is the velocity operator. Hence

$$V_{mn} = \frac{e}{L} v_{mn} = \frac{e}{L} (E_m - E_n)^2 r_{mn}, \quad (14)$$

where r is the position operator. Thus an LRT or an SLRT study of the conductance reduces to a study of the statistical properties of the so-called dipole-matrix elements. These statistical properties become nontrivial for either weak or strong disorder and they should be described by a *non-Gaussian ensemble. The following subsections contain some extra details regarding metallic rings and can be skipped in first reading.*

A. Characterization of metallic rings

A metallic ring is characterized by the Fermi velocity v_E, the Fermi momentum k_E, the length of the ring L, its width $L_\perp$, and the strength of the disorder W. The latter determines the mean-free path ℓ. The Fermi velocity v_E can be regarded as providing conversion between "length" and "time" hence we have two dimensionless parameters: the number of open modes $\mathcal{M} \sim (k_E L_\perp)^{d-1}$ and the degree of disorder L/ℓ. For-
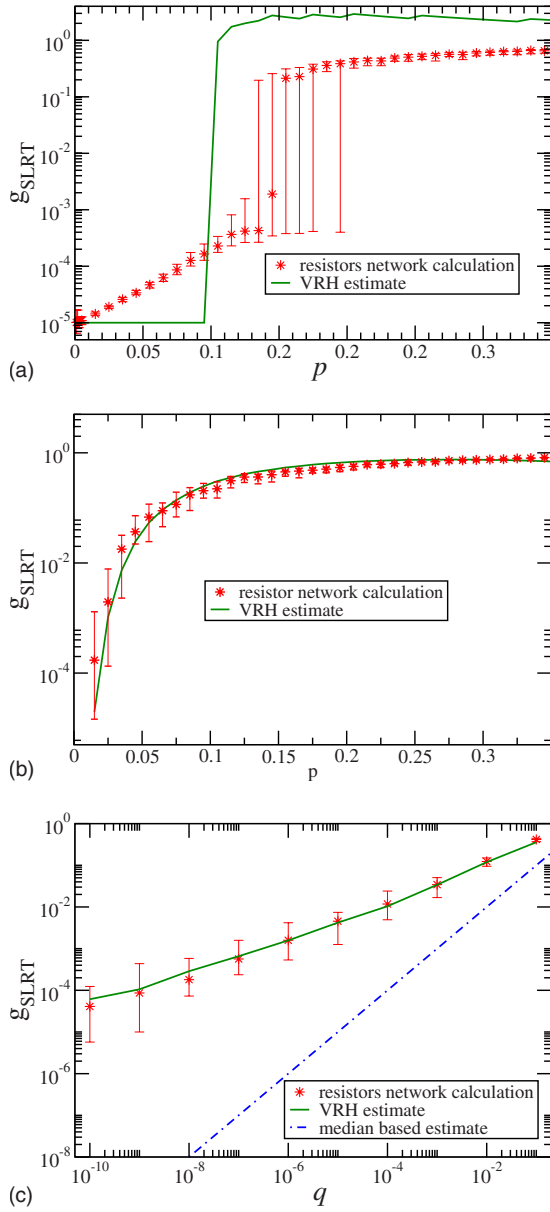
FIG. 3. (Color online) The SLRT suppression factor g_{SLRT} versus the sparsity parameter (p or q) for bimodal distribution with rectangular power spectrum (upper panel); (log-box distribution with exponential power spectrum (middle panel); and log-normal distribution with rectangular power spectrum (lower panel). The resistor network and the VRH calculation were done for 100 realizations of 256×256 matrices with $b = 10$. In the bimodal case VRH is not satisfactory. In the log-normal case the VRH result is contrasted with the naive median based estimate.
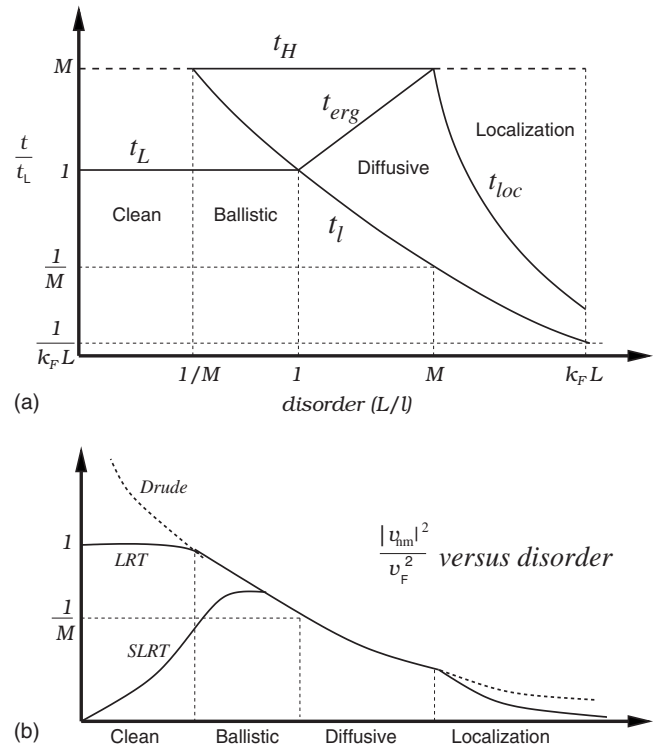

FIG. 4. Upper panel: time scales versus the disorder strength (see Sec. II A). Lower panel: schematic illustration that sketches the dependence of the dc conductance on the strength of the disorder. It should be regarded as a caricature of Fig. 2.

mally there is a third independent dimensionless parameter $k_E L$ but we assume it to be very large compared with $\mathcal{M}$ and hence it has no significant role in the analysis below. The various regimes in this problem are described below and in the diagram of Fig. 4: (a) clean ring $(L/\ell) < 1/\mathcal{M}$, (b) ballistic ring $(L/\ell) < 1$, (c) diffusive ring $(L/\ell) > 1$, and (d) Anderson regime $(L/\ell) > \mathcal{M}$.

It is a matter of terminology whether to exclude the "clean" case from the ballistic regime and the "Anderson" case from the "diffusive" regime. The time scale which is

associated with the length of the rings is $t_L = L/v_E$, the time scale which is associated with the scattering is mean-free time $t_\ell = \ell/v_E$, and the time scale which is associated with quantum recurrences is the Heisenberg time $t_H = \mathcal{M} t_L$. If the very strong condition $t_\ell > t_H$ is satisfied then we call it "clean ring" meaning that the disorder does not mix the levels and its effect can be treated using first-order perturbation theory.

More generally we define the ballistic regime by the condition $\ell \gg L$. If the disorder is strong enough then the levels are mixed nonperturbatively leading to genuine semiclassical ballistic behavior with

$$t_L < t_\ell < t_H \quad \text{[Ballistic]}. \quad (15)$$

In the diffusive regime it is meaningful to define the ergodic (Thouless) time via the relation $D_0 t \sim L^2$ where $D_0 = v_E \ell$, leading to $t_{erg} = (L/\ell) t_L$. In the strict diffusive regime we have

$$t_\ell < t_{erg} < t_H \quad \text{[Diffusive]}. \quad (16)$$

If we have (formally) $t_{erg} > t_H$ then there is no ergodization but rather a strong (Anderson) localization effect shows up. This means that one expects a breaktime t_{loc} that marks a crossover from diffusion to saturation. A standard argumentation (see below) gives the estimate $t_{loc} = \mathcal{M}^2 t_\ell$. One observes that in the Anderson regime

$$t_\ell < t_{loc} < t_H \quad \text{[Anderson]}. \quad (17)$$

The self-consistent determination of ℓ_ξ originates in old studies of dynamical localization in the quantum kicked rotator problem. Assuming that the localization length is ℓ_ξ, the lo-

cal level spacing is $\Delta_\xi = \pi v_E / \mathcal{M} \ell_\xi$, and hence the breaktime is $t_{loc} = 2\pi / \Delta_\xi$. The self-consistency condition is $D t_{loc} \sim \ell_\xi^2$, leading to

$$\ell_\xi \approx \mathcal{M} \ell. \qquad (18)$$

The identification of the Anderson regime is via the requirement $L > \ell_\xi$. Finally we note that the largest meaningful value of disorder is $(L/\ell) = k_E L$, for which ℓ equals the Fermi wavelength.

B. Kubo-Drude conductance

The coefficient G is defined through the expression $D_E = G \varepsilon^2$ for the one-particle diffusion coefficient, where ε is the RMS of the voltage. Taking Eq. (14) into account it follows that

$$G = \pi \varrho_E \times \left(\frac{e}{L} \right)^2 \langle\langle |v_{mn}|^2 \rangle\rangle. \qquad (19)$$

The Ohmic conductance is defined as the coefficient in the Joule formula $G_{Ohm} \epsilon^2$ for the rate of energy absorption. For an $\mathcal{N}$ particle system at temperature T it is related to G via a general diffusion-dissipation relation

$$G_{Ohm} = \varrho_E \times G \quad \text{[Fermi]}, \qquad (20)$$

$$G_{Ohm} = (\mathcal{N}/T) \times G \quad \text{[Boltzmann]}. \qquad (21)$$

The Boltzmann occupation applies to semiconductors, where $\mathcal{N}/L$ is the density of the particles. For Fermi occupation ϱ_E / L is the density of states at the Fermi energy per unit length of the ring and it is in agreement with the Boltzmann result if we regard $\mathcal{N} = \varrho_E T$ as the effective number of carriers.

In the case of a diffusive ring it makes sense to relate the diffusion in energy to the diffusion in real space. This relation holds in the strict dc limit. Using the Einstein relation $G_{Ohm} = (e/L)^2 \varrho_E \mathcal{D}$ we deduce that

$$\mathcal{D} = \pi \varrho_E \times \langle\langle |v_{mn}|^2 \rangle\rangle_{\omega_c \sim 0}. \qquad (22)$$

It is important to keep in mind that for a disconnected ring $\mathcal{D} = 0$ but still we can get from Eq. (22) a nonzero result $G \neq 0$ because the spectral content of the driving may have a finite cut-off frequency ω_c.

The reference case for all our calculations is the Drude result which is obtained for a diffusive ring in the semiclassical approximation (see Appendix C). Assuming a mean-free path ℓ we write the Drude result as

$$G_{Drude} = \frac{e^2}{2\pi\hbar} \mathcal{M} \frac{\ell}{L}, \qquad (23)$$

where L is the length of the ring and $\mathcal{M}$ is the number of open modes (proportional to its cross section).

The quantum Kubo calculation gives in leading order the same result as Drude: this is well known and obviously it is also a by-product of the subsequent analysis. One observes that the there is a *maximum* Kubo conductance which is obtained in the limit of a clean ring, i.e., for $\ell/L = \mathcal{M}$. For completeness we note that for a ring with transmission g_0,

the following formal identification applies (see Appendix C):

$$\frac{\ell}{L} \Leftrightarrow \frac{g_0}{1 - g_0} \quad [< \mathcal{M}]. \qquad (24)$$

This makes transparent the relation between the Drude and the Landauer results.

In later sections our interest is to find the SLRT suppression factor g_{SLRT} that determines the ratio G_{Ohm}/G_{Drude}. For this purpose we have to find not only the average value of $|v_{mn}|^2$ but also their statistics.

III. RMT MODELING

Regarded as a random matrix V_{mn} is characterized by its band profile and by the size distribution of its elements. The standard RMT modeling due to Wigner assumes either full or banded matrix with elements that are taken out of a Gaussian distribution. But our interest is in circumstances where the size distribution is wide, i.e., the elements of $|V_{mn}|^2$ look like realizations of a random variable x whose logarithmic value $[\log(x)]$ is distributed over several decades.

In practice the $|V_{mn}|^2$ of a physical model does not have an idealized flat band profile. Consequently, we write

$$|V_{mn}|^2 = X_{mn} \times \tilde{C}(E_m - E_n), \qquad (25)$$

where $\tilde{C}(\omega)$ describes the band profile of the matrix. Numerically the band profile is obtained by averaging separately each diagonal $[(n-m) = \text{const}]$ of the matrix and plotting the result against $\omega = (E_n - E_m) \approx (n-m) \varrho_E^{-1}$.

The question arises, given a matrix A_{mn} that consist of real non-negative elements, how to numerically define its band-width b, its sparsity s, and the associated distribution $\rho(x)$ of its in-band elements. For the purpose of this paper it was important to adopt an unambiguous definition of s, which loosely speaking is defined as the percentage of large in-band elements. The suggested procedure below is based on the participation number (PN) concept. The PN of a set $\{x_i\}$ is defined as

$$PN = \frac{\left(\sum_i x_i \right)^2}{\sum_i x_i^2} \qquad (26)$$

and reflects the number of the large elements. The procedure to determine s and b goes as follows: (1) we consider a truncated A_{mn} within the energy window of interest. (2) We calculate the band profile by averaging separately the elements over each diagonal. (3) We construct an untextured matrix A_{mn}^{utx} by performing random permutations of the elements along the diagonals. (4) We construct a uniformized matrix A_{mn}^{unf} by replacing each of the elements of a given diagonal by their average. (5) We calculate the participation number of the elements in A_{mn}. This is like counting the number of large elements. (6) We calculate the participation number of the elements in A_{mn}^{unf}. This is like counting the number of in-band elements. (7) The ratio of the numbers that have been calculated in the previous step is defined as

the sparsity s. (8) Likewise the bandwidth b is deduced from the number of in-band elements.

The size distribution $\rho(x)$ refers to the in-band elements. In order to verify that A_{mn} is really like a random matrix we perform the SLRT calculation (see Sec. IV) once on A_{mn} and once on the untextured matrix A_{mn}^{utx}. If the results are significantly different we say that texture, i.e., the nonrandom arrangement of the large elements, is important. The RMT analysis in this paper assumes that texture is not too significant.

In particular, we are interested in the bimodal, log-box, and log-normal ensembles. The *bimodal distribution* is characterized by the probability p of having a large value $x=x_1$, otherwise $x=x_0 \ll x_1$, hence

$$\rho(x) = (1-p)\delta(x-x_0) + p\,\delta(x-x_1). \quad (27)$$

In the case of a *log-box distribution* the variable $\ln(x)$ has uniform distribution within $[x_0, x_1]$, hence

$$\rho(x) = \frac{1}{\ln(x_1/x_0)}\frac{1}{x}. \quad (28)$$

In the case of a *log-normal distribution* the variable $\ln(x)$ has a Gaussian distribution with mean $\ln(x_0)$ and standard deviation σ, hence

$$\rho(x) = \frac{1}{\sqrt{2\pi}\sigma}\frac{1}{x}e^{-[\ln(x/x_0)]^2/2\sigma^2}. \quad (29)$$

A random variable can be characterized by the algebraic, geometric and harmonic averages

$$\langle\langle x \rangle\rangle_a = \langle x \rangle, \quad (30)$$

$$\langle\langle x \rangle\rangle_g = \exp[\langle \ln x \rangle], \quad (31)$$

$$\langle\langle x \rangle\rangle_h = [\langle 1/x \rangle]^{-1}. \quad (32)$$

The sparsity of a matrix that consists of uncorrelated realizations can be characterized by a parameter s or optionally by the parameters p and q that are defined as follows:

$$s = \langle x \rangle^2 / \langle x^2 \rangle, \quad (33)$$

$$p = \text{Prob}(x > \langle x \rangle), \quad (34)$$

$$q = \langle\langle x \rangle\rangle_{\text{median}} / \langle x \rangle. \quad (35)$$

By this definition p is the fraction of the elements that are larger than the algebraic average and q is the ratio between the median and the algebraic average. We regard a matrix as sparse if $s \ll 1$ or equivalently if $p \ll 1$ or $q \ll 1$.

IV. SLRT CALCULATION

As in the standard derivation of the Kubo formula, also within the framework of SLRT, the leading mechanism for absorption is assumed to be FGR transitions. These are proportional to the squared matrix elements $|V_{mn}|^2$. The power spectrum of $\dot{f}(t)$ is $\widetilde{S}(\omega) = \varepsilon^2 \widetilde{F}(\omega)$, where ε is the RMS value

of the driving amplitude. Consequently, the FGR transition rates are

$$w_{mn} = 2\pi \frac{|V_{mn}|^2}{(E_m - E_n)^2}\widetilde{S}(E_m - E_n). \quad (36)$$

From Eqs. (1), (25), and (36) one deduces the identification

$$\widetilde{B}(\omega) = \frac{2\pi}{\omega^2}\widetilde{C}(\omega)\widetilde{S}(\omega). \quad (37)$$

The inverse resistivity of the network has the meaning of diffusion coefficient and from the definition of G in Eq. (3) we deduce the SLRT *formula* Eq. (5) with

$$\langle\langle |V_{mn}|^2 \rangle\rangle \equiv \left[\left[2\varrho_E^{-3}\frac{|V_{mn}|^2}{(E_m-E_n)^2}\widetilde{F}(E_m-E_n)\right]\right]. \quad (38)$$

This should be contrasted with the *Kubo formula* that involves an algebraic instead of SLRT average

$$\langle\langle |V_{mn}|^2 \rangle\rangle_a \equiv \left[\varrho_E^{-1}\sum_m |V_{mn}|^2 \widetilde{F}(E_m-E_n)\right]_{\text{avr}} \quad (39)$$

with average over the reference state n. The average is done over all the states whose energy E_n is within the energy window of interest. In the metallic context it is an average around the Fermi energy.

It is a simple exercise to verify that if all the matrix elements are the same, say $|V_{mn}|^2 = c_0$, then $\langle\langle |V_{mn}|^2 \rangle\rangle = c_0$ too. Also it is a simple exercise to verify that the SLRT formula coincides with the Kubo formula if there is no randomness, i.e., if $|V_{mn}|^2$ is a well-defined function of $E_m - E_n$. But if the matrix is structured or sparse then

$$\langle\langle |V_{mn}|^2 \rangle\rangle_h < \langle\langle |V_{mn}|^2 \rangle\rangle \ll \langle\langle |V_{mn}|^2 \rangle\rangle_a. \quad (40)$$

If only neighboring levels are coupled then "adding resistors in series" (see Appendix A) implies equality of the SLRT average to the harmonic average

$$\langle\langle |V_{mn}|^2 \rangle\rangle_h \equiv \left[\varrho_E^{-1}\sum_m \frac{1}{|V_{mn}|^2}\widetilde{F}(E_m-E_n)\right]_{\text{avr}}^{-1}. \quad (41)$$

More generally the harmonic average is a gross underestimate. A generalized VRH scheme that we present in Sec. V provides the following approximation for the SLRT average:

$$\langle\langle |V_{mn}|^2 \rangle\rangle \sim [\varrho_E^{-1}[|V_{mn}|^2]_\omega \widetilde{F}(\omega)]_{\text{max}}, \quad (42)$$

where the maximum is calculated with respect to ω. The typical value $|V_{mn}|_\omega^2$ for ω transitions will be defined precisely in Sec. V and it reflects the size distribution of the matrix elements. The VRH integral Eq. (6) is an *ad hoc* refinement of Eq. (42) that better interpolates with the LRT result and therefore it is advantageous for actual numerical analysis. Further analysis (see Sec. VI) indicates that compared with the weighted harmonic average $\langle\langle |V_{mn}|^2 \rangle\rangle_h$, of Eq. (41), the corresponding geometric average $\langle\langle |V_{mn}|^2 \rangle\rangle_g$ provides in most cases a better lower bound.

V. GENERALIZED VRH APPROXIMATION

A 1D network is characterized by its inverse resistivity $w = [[w_{mn}]]$. Inspired by Ref. 6, the inverse resistivity can be

estimated analytically by finding the maximum threshold such that the elements $w_{mn} > w_0$ form a *connected cluster*. This leads in the present context to a generalized VRH estimate which we explain in the following paragraph.

Given a threshold w and truncating the bandwidth at ω, a sufficient condition for having a connected cluster is to have at least one nonzero element per ω segment

$$\varrho_{\mathrm{E}}\omega \times \mathrm{Prob}[x\widetilde{B}(\omega) > w] \quad \text{larger than unity.} \quad (43)$$

We define the typical value x_ω for range ω transitions via the relation

$$\varrho_{\mathrm{E}}\omega \times \mathrm{Prob}(x > x_\omega) \sim 1 \quad (44)$$

and rewrite the condition for having a connected cluster in the following suggestive form:

$$w < x_\omega \widetilde{B}(\omega). \quad (45)$$

Thus an underestimate for the diffusion coefficient is $D \sim w\omega^2$ based on hopping rate w with steps ω. The VRH estimate is based on the idea to optimize this underestimate with respect to ω and w, leading to

$$D_{\mathrm{E}} \sim [\omega^2 x_\omega \widetilde{B}(\omega)]_{\max}, \quad (46)$$

where the maximum is with respect to the hopping range ω. In the FGR context this leads to Eq. (42) with

$$[|V_{mn}|^2]_\omega \equiv x_\omega \widetilde{C}(\omega). \quad (47)$$

VI. SLRT ANALYSIS OF SOME PROTOTYPE NON-GAUSSIAN ENSEMBLES

In this section we derive results for SLRT suppression factor g_{SLRT} for the bimodal, for the log-box, and for the log-normal ensembles. The bimodal distribution is the simplest for pedagogical purpose while the log-box and log-normal ensembles are of greater physical relevance. The main results are summarized below while further details of the calculation are given in Appendices D and E. Figure 3 presents the outcome of numerical analysis that tests the accuracy of the generalized VRH approximation. In later sections we shall see that the presented results are of relevance to the study of conductance in the limits of strong and weak disorders.

The bimodal ensemble. In this case there is a minority of large elements ($x=x_1$) that have percentage $p \ll 1$ and a majority of small elements ($x=x_0 \ll 1$) that have percentage $1-p$. Consequently, the typical value for ω transition has a percolationlike crossover from $x_\omega=x_0$ to $x_\omega=x_1$ at the frequency $\omega=(\varrho_{\mathrm{E}}p)^{-1}$. Therefore

$$g_{\mathrm{SLRT}} \sim \begin{cases} q\widetilde{F}(\omega \sim 0) & bp < 1 \\ (1/p)\widetilde{F}[1/(\varrho_{\mathrm{E}}p)] & bp > 1, \end{cases} \quad (48)$$

where $b=\varrho_{\mathrm{E}}\omega_c$ is the dimensionless bandwidth and $q \approx x_0/(px_1)$. The first expression reflects the possibility of *majority dominance* of the small elements while the second expression reflects the possibility of *minority dominance* of

the large elements. Note that the VRH approximately implicitly assumes that $F(\omega)$ drops (say) exponentially such that $g_{\mathrm{SLRT}} \leq 1$, otherwise the result cannot be trusted.

The log-box ensemble. In this case the probability distribution of $\ln(x)$ is uniform over many decades. Therefore, it is reasonable to assume that the result for g_{SLRT} is *minority dominated*. It is natural to characterize the log-box distribution of Eq. (28) by a parameter $\tilde{p}=[\ln(x_1/x_0)]^{-1}$, and to realize that the percentage of large elements is $p \approx -\tilde{p}\ln\tilde{p}$. Note that the corresponding sparsity parameter is $s \approx 2\tilde{p}$. The typical value for ω transitions is

$$x_\omega \approx \frac{1}{\tilde{p}}\exp\left(-\frac{1}{\tilde{p}\varrho_{\mathrm{E}}\omega}\right)\langle\langle x \rangle\rangle_{\mathrm{a}} \quad (49)$$

and the VRH estimate, assuming an exponential bandprofile gives

$$g_{\mathrm{SLRT}} \sim \frac{1}{\tilde{p}}\exp\left[-2\left(\frac{1}{\tilde{p}b}\right)^{1/2}\right]. \quad (50)$$

Note the similarity, as well as the subtle difference, compared with the bimodal minority dominance expectation.

The log-normal ensemble. In this case the probability distribution of $\ln(x)$ is a Gaussian centered around the median. Therefore, it is reasonable to assume that the result for g_{SLRT} is *majority dominated*. It is natural to characterize the log-normal distribution of Eq. (29) by a parameter q, which is defined as the ratio of the median to the algebraic average. Note that the corresponding sparsity parameter is $s=q^2$. The VRH calculation gives the result

$$g_{\mathrm{SLRT}} \sim q\exp\left\{\left[\mathrm{factor} \times \ln\left(\frac{1}{q}\right)\ln(b)\right]^{1/2}\right\}, \quad (51)$$

where the factor is determined by the band profile (it is 2 for an exponential bandprofile and 4 for a rectangular bandprofile). Note that $g_{\mathrm{SLRT}} \sim q$ is the simplest guess that reflects the majority dominance expectation.

VII. SEMICLASSICAL ESTIMATE OF THE OHMIC CONDUCTANCE

There is a well-established semiclassical procedure to deduce the algebraic average of the matrix elements $|V_{mn}|^2$ that correspond to the energy difference $\omega=E_m-E_n$ from the associated correlation function $\langle V(t)V(0)\rangle$. We would like to apply this procedure in order to estimate the conductance of metallic rings. Hence our interest is in the matrix elements of the velocity operator. The semiclassical estimate is based on the following observation:

$$\langle\langle|v_{mn}|^2\rangle\rangle_\omega = \frac{1}{2\pi\varrho_{\mathrm{E}}}\mathrm{FT}[\langle v(t)v(0)\rangle], \quad (52)$$

where FT stands for Fourier transform. The velocity-velocity correlation function can be obtained via a time derivative of the time-dependent diffusion coefficient $\mathcal{D}(t)$, which is the time derivative of the spreading $\langle[r(t)-r(0)]^2\rangle$.

In the Drude "classical" approximation one assumes an exponential decay of the velocity-velocity correlation func-

tion and long-time diffusion $\mathcal{D}_0$ as determined by the mean-free path (see Appendix C). This is satisfactory in the ballistic and diffusive regimes, and leads to a Lorentzian line shape

$$\langle\langle |v_{mn}|^2 \rangle\rangle_\omega = \frac{1}{b}v_{\rm E}^2 \frac{R(\omega)}{1+(t_\ell\omega)^2}, \tag{53}$$

where $b=\mathcal{M}L/\ell$ is the dimensionless bandwidth of the matrix and $R(\omega)=1$.

But in the Anderson regime we know that there is a break-time $t_{\rm loc}$ that marks the crossover form diffusion to localization and hence for a bulk system formally $\mathcal{D}=0$. Consequently, the FT consideration of Eq. (53) leads to the conclusion that in the limit $\omega\to 0$ the band profile should vanish if the system is infinite. The simplest reasoning[9] leads to the expression

$$R(\omega) = \frac{L}{\ell_\xi}e^{-2L/\ell_\xi} + \frac{1}{1+(t_{\rm loc}\omega)^{-2}}, \tag{54}$$

where the first term reflects the finite length of the system and it is deduced using Eq. (24). We shall see in Sec. IX, using a different more refined approach, that the second term is almost correct. Namely, the more careful analysis using the Mott's picture predicts that the small frequency dependence is not $[\omega]^2$ but $[\omega \log(\omega)]^2$.
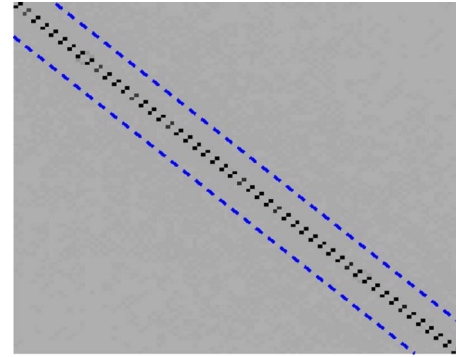
The quantum-mechanical analysis should further take into account (i) the statistics of the levels and (ii) the fluctuations in the size of the matrix elements. The former implies wiggles in $R(\omega)$ for small frequencies while the latter imply that the average size of the matrix elements does not necessarily reflect their typical value. Figure 4 summarizes the dependance of the matrix elements on the disorder.

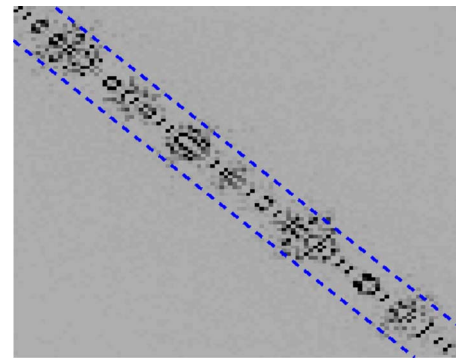It should be clear that we always have the sum rule

$$\sum_m |v_{mn}|^2 = v_{\rm E}^2. \tag{55}$$

In the clean ring limit the sum is dominated by the diagonal or near diagonal element while all the other off-diagonal elements become negligible. Still the estimate Eq. (53) for the other off-diagonal matrix elements remains valid and can be justified using first-order perturbation theory. If the ring is ballistic (but not clean) then the semiclassical estimate Eq. (53) implies that the large elements form a band of width $b>1$. If the matrix is not sparse then the contribution of all the b in-band elements to the sum rule is comparable. But if (say) only a fraction $s\ll 1$ of of elements are contributing then their typical value $|v_{mn}|^2 \sim \langle\langle |v_{mn}|^2 \rangle\rangle_\omega/s$ is much larger compared with the average. We shall come back to a more detailed discussion of "sparsity" in the subsequent sections.

In the diffusion regime $R(\omega)$ mainly reflects the level-spacing statistics of the individual levels, which is a "microscopic" effect that leads to small weak-localization corrections that had been studied extensively.[19,20] But in the strong-localization Anderson regime the implication of the breaktime leads to the dramatic conclusion that $R(\omega)\ll 1$ for $\omega\ll\Delta_\xi$, where the local level spacing Δ_ξ is *not* related to the volume-dependent microscopic level spacing $\varrho_{\rm E}^{-1}$ but to the strength of the disorder.

(a)

(b)

FIG. 5. (Color online) Images of 100×100 pieces of the perturbation matrix $|v_{nm}|^2$ in the clean ($W=0.001$) and ballistic ($W=0.1$) regimes. The dashed lines correspond to the ballistic bandwidth $\mathcal{M}=10$, which is associated with the time scale t_L.

In the Anderson regime it is evident that $\langle\langle |v_{mn}|^2 \rangle\rangle_\omega$ is not the typical value of the matrix elements. Roughly speaking and disregarding the ω dependence

$$|v_{mn}| \sim \frac{v_{\rm E}}{\mathcal{M}}\exp\left(-\frac{|r|}{\ell_\xi}\right), \tag{56}$$

where $r\in[0,L/2]$ has a uniform distribution, implying a log-box distribution for the size of the elements. Accordingly, the typical value is exponentially small in the length of the ring while the average is determined by the small percentage of large elements and comes out in agreement with the semiclassical estimate. In Sec. IX we further elaborate on the statistical analysis of the sparsity in the Anderson regime using the Mott's picture of localization.

VIII. RMT STATISTICS IN THE BALLISTIC REGIME

For zero disorder $W=0$ each energy level is doubly degenerate in the basis of real eigenfunctions and the couplings are pairwise, i.e., the matrix element between states of different energies is zero. See Fig. 5. Consequently, the EMF cannot induce connected sequences of transitions and the SLRT conductance should be zero. The nonzero elements of the perturbation matrix according to the sum rule [Eq. (55)] are $|v_{nm}|=v_{\rm E}$. The algebraic average of the near diagonal elements equals this value (of the large size elements) multiplied by their percentage $p_0\approx 1/2$. Consequently
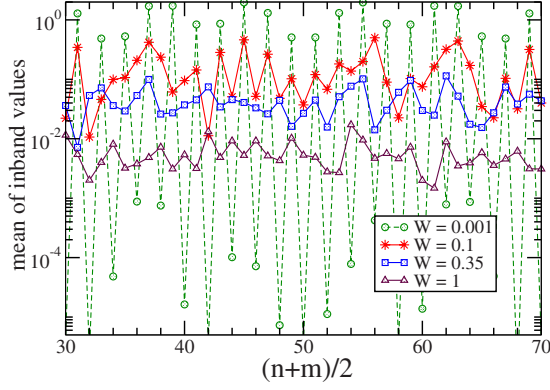
FIG. 6. (Color online) The mean of the in-band values of the $|v_{nm}|^2$ matrix elements as a function of $(n+m)/2$ for different values of disorder. The pronounced modulation in the ballistic regime is an indication for texture.

$$\langle\langle |v_{nm}|^2 \rangle\rangle_a \approx \frac{1}{2}v_F^2. \qquad (57)$$

For sufficiently small W these large-size matrix elements are not affected, and therefore, the algebraic average stays the same. Consequently, in the clean-ring limit the Kubo conductance is formally finite and attains the maximal value as discussed with regard to Eq. (23).

In the clean as well as in the whole ballistic regime the algebraic average $\langle\langle |v_{mn}|^2 \rangle\rangle_\omega$ does not reflect the sparsity and the textures of the v_{mn}. See Figs. 6 and 7. When we look on the image of v_{mn} the immediate reaction is to be impressed by the *texture* and therefore we discuss it first. Subsequently, we discuss the *sparsity*, which is in fact more significant for the analysis.

The mean DOS of the two-dimensional ring is ϱ_E. But $L_x \gg L_y$ and, therefore, it is not uniform. As the disorder W is increased, levels start to mix first in the high DOS regions, and only later in the low DOS regions. This is the reason for the appearance of textures. Let us be more detailed about the
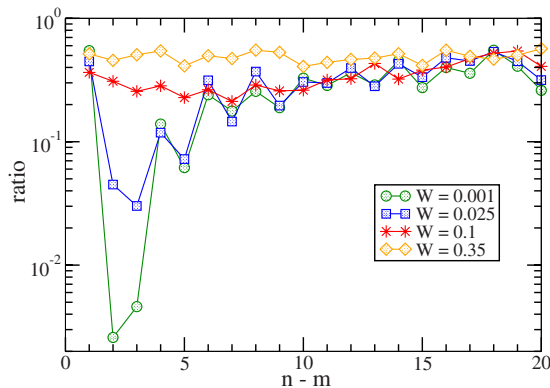

FIG. 7. (Color online) The ratio between the typical value $[|v_{nm}|^2]_\omega$ and the average value $\langle |v_{nm}|^2 \rangle_\omega$ that enter into Eqs. (6) and (4), respectively. In this plot the typical value is the median. The horizontal axis is $n-m$ corresponding to the scaled frequency $\varrho_E\omega$. Note that both $[|v_{nm}|^2]_\omega$ and $\langle |v_{nm}|^2 \rangle_\omega$ when plotted as a function of ω have a Lorentzian line shape.

nonuniformity of the DOS. As a function of the energy E each time that a mode is opened the DOS is boosted. Consequently, ϱ_E is modulated. This systematic modulation is associated with the opening of a single additional mode at every threshold energy and, therefore, scales like $1/\mathcal{M}$. On top there is an additional weaker nonsystematic modulation of the DOS because the levels of low-density modes add up to the levels of the high-density modes. It is the latter type of modulation which is reflected in Figs. 5 and 6, where the energy window contains throughout exactly ten open modes.

In the regions where levels are not yet mixed one can estimate the majority of small matrix elements using first-order perturbation theory: Due to the first-order mixing of the levels, the typical overlap $|\langle \boldsymbol{m} | n \rangle|$ between perturbed and unperturbed states is

$$|\langle \boldsymbol{m} | n \rangle| = \left| \frac{U_{nm}}{E_n - E_m} \right|. \qquad (58)$$

The typical size of a small v_{nm} element is the multiplication of this overlap, calculated for $(E_n - E_m) \sim \varrho E^{-1}$, by the size of the nonzero $|v_{nm}| = v_E$ element. As *a priori* expected this first order estimate gives a result that agrees with the semiclassical estimate Eq. (53) evaluated for $\omega \sim \varrho_E^{-1}$. Thus

$$q \approx \mathcal{M}\frac{L}{\ell} \quad \text{[for white disorder]}. \qquad (59)$$

Above some threshold, first-order perturbation theory fails everywhere, meaning that nonperturbative mixing takes place in any energy. Still, due to the modulation of the DOS, the mixing range is wider in the near-thresholds energies and therefore the matrix elements there are *smaller*. So now we have the opposite situation, of *high*-DOS *bottleneck* instead of *low*-DOS *bottleneck*.

One easily observes that the crossover from weak disorder (that features separated mixing regions and low-DOS bottlenecks) to stronger disorder (that features a connected mixing region and high-DOS bottlenecks) is associated with the crossover from the clean to the ballistic regime. The width of the crossover region depends on the nonuniformity of the DOS and therefore diminishes as the number of open modes becomes large.

The above reasoning implies that the texture might be important in the SLRT analysis primarily in the clean ring regime but much less in the genuine ballistic regime. But what about sparsity? Using the FGR in order to determine the energy range over which mixing takes place, we obtain an estimate for the bandwidth of the perturbation matrix

$$b = 2\pi\varrho_E^2 |U_{nm}|^2 \approx \mathcal{M}\frac{L}{\ell}, \qquad (60)$$

which agrees with the semiclassical estimate. But in the ballistic regime $b < \mathcal{M}$. This means that a typical eigenstates cannot occupy all the $\mathcal{M}$ open modes. Rather it has there a participation number $M = b$ smaller than $\mathcal{M}$ (see Fig. 2). Consequently, we deduce that the sparsity of the perturbation matrix is
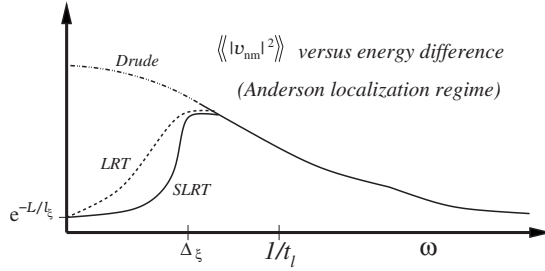
FIG. 8. Schematic plot that illustrates the dependence of the average and the typical values of the matrix elements on the energy separation ω. These are labeled as "LRT" and "SLRT," respectively, and compared with the semiclassical (Drude) expectation. The plot refers to the Anderson regime. For a corresponding numerical illustration in the ballistic regime see Fig. 7.

$$s = \frac{M}{\mathcal{M}} \approx \frac{L}{\ell} \equiv q^2 \quad \text{[for smooth disorder],} \quad (61)$$

where the identification of s with q^2 is based on the assumption of a log-normal distribution which we further discuss in the next paragraph. Unlike the texture, the sparsity persists via the whole ballistic regime up to the border with the diffusive regime. For this reason we regard the sparsity as the main ingredient in the SLRT analysis.

The discussion of sparsity in the previous paragraph is somewhat meaningless unless one specifies the distribution to which s refers. At this point of the discussion it is essential to distinguish between *white disorder* for which the scattering is isotropic and *smooth disorder* for which only nearby modes are coupled (small scattering angle). The latter applies if the potential floor within the ring has a smooth rather than erratic variation with respect to the Fermi wavelength. Assuming smooth disorder it becomes essential to extend the perturbation theory of Appendix B beyond first order. It makes sense to say that $|v_{mn}| \sim |W|^r$, where the order r is bounded by $\mathcal{M}$. Therefore, $\log(|v_{mn}|)$ has some bounded distribution which can be approximated (say) by a Gaussian. It follows that a log-normal ensemble should be qualitatively appropriate to describe the statistical properties. It follows that g_{SLRT} can be estimated using Eq. (51) with the q of Eq. (61). On the other hand in the case of white disorder $|v_{mn}|$ of the majority elements is given by *first*-order perturbation theory and then one should use Eq. (51) with the q of Eq. (59).

IX. RMT STATISTICS IN THE ANDERSON REGIME

The simplest picture of localization regards the lattice as composed of segments of size ℓ_ξ and assumes that each eigenstate is well localized in one of this segments. Accordingly, non-negligible matrix elements are only between states that reside in the same space segment. We shall refer to this as the "zero-order" picture. Taking into account that the matrix element of the velocity operator are related to those of the position operator by the relation $|v_{mn}|^2 = \omega^2 |r_{mn}|^2$, it follows that $R(\omega) \sim (\omega/\Delta_\xi)^2$ in consistency with the semiclassical reasoning of Sec. VII, which is summarized by Fig. 8.

In order to refine this picture we use the following procedure due to Mott. The zero-order basis is determined by ignoring the possibility of the particle to hop from segment to segment. In order to find the "true" eigenstates we have to take into account the residual interaction. It is reasonable to postulate that if the distance between two zero-order eigenstates is $r = r_n - r_m$ then the residual interaction is

$$\kappa = \Delta_\xi \exp(-|r|/\ell_\xi). \quad (62)$$

The prefactor is the natural educated guess, which is later justified (see below) by requiring consistency with the semiclassical result.

If we have two zero-order eigenstates that do not reside at the same segment but have distance r in space and distance ε in energy then the true eigenstates have energy difference $\omega = \sqrt{\varepsilon^2 + \kappa^2}$ and the dipole-matrix element becomes $|r_{mn}| = (\kappa/\omega) \times (r/2)$ instead of zero. Originally the zero-order eigenstates had a density $(\varrho_E/L)d\varepsilon dr$ but now the region $|\varepsilon| < \exp(-|r|/\ell_\xi)$ is depleted and forms a density $d\omega/\Delta_\xi$ of so-called Mott resonant states. If we slice all those states that have energy difference ω then

$$|v_{mn}| \sim \begin{cases} \Delta_\xi r e^{-|r|/\ell_\xi} & \text{off res} \\ |\omega| r_\omega & \text{on res,} \end{cases} \quad (63)$$

where

$$r_\omega = \ell_\xi \log(\Delta_\xi/\omega). \quad (64)$$

This implies that the size distribution of the $|v_{mn}|$ elements that reside inside a band of width ω is within

$$\frac{v_E}{\mathcal{M}} \times \left[\frac{L}{\ell_\xi} e^{-L/\ell_\xi}, \; 1 \right] \quad \text{for } |\omega| > \Delta_\xi \quad (65)$$

$$\frac{v_E}{\mathcal{M}} \times \left[\frac{L}{\ell_\xi} e^{-L/\ell_\xi}, \; \frac{\omega}{\Delta_\xi} \log\left(\frac{\Delta_\xi}{\omega} \right) \right] \quad \text{for } |\omega| < \Delta_\xi. \quad (66)$$

Compared with Eq. (54) this is a refinement that takes properly into account the ω dependence of the matrix elements. Disregarding a logarithmic correction it reproduces the semiclassical result Eq. (53).

If we ignore the Mott resonant states, then a log-box distribution is implied. The Mott resonant states form a *box* distribution on top. In a log scale the Mott resonant states contributes a peak of large elements. But this peak does not affect the x_ω calculation. Consequently, for practical purpose we can regard the matrix elements in the SLRT calculation as having a simple log-box distribution as reflected by the crude approximation of Eq. (56). The sparsity of this distribution is characterized by

$$\tilde{p} = \mathcal{M} \frac{\ell}{L} \quad (67)$$

and the SLRT suppression factor is given by Eq. (50).

X. SLRT VS VRH CALCULATION

In order to appreciate the similarities and the differences between SLRT and the conventional Hopping calculation, we

cast the latter into the SLRT language. Equation (4.4) of Ref. 6 for the dc hopping conductance due to phonon-induced transitions is

$$G_{\mathrm{Ohm}} = \frac{1}{\mathcal{N}} \left[\left[\frac{e^2}{T} [1 - f(E_n)] f(E_m) w_{mn}^\gamma \right] \right]_{\parallel}. \quad (68)$$

The notation $[[\dots]]_{\parallel}$ implies that the resistance of the network is calculated between states at the same energy $E \sim E_{\mathrm{E}}$ that reside in opposite sides of the sample. Due to the Fermi occupation factor, the network contains effectively $\mathcal{N} = \varrho_{\mathrm{E}} T$ nodes. The division by $\mathcal{N}$ is required because we have defined the $[[\dots]]$ as inverse resistivity and not as inverse resistance of the network.

The occupation factor $[1 - f(E_n)] f(E_m)/T$ gives $\mathcal{O}(1)$ weight only to the $\mathcal{N}$ levels that reside within a window of width T. If we ignore the relaxation effects and regard the fluctuating environment as a noise source that induces transitions $w_{mn}^\gamma \propto \exp(|E_m - E_n|/T)$, we still should get the same result for G, even if we omit the occupation factor. This point of view allows to bridge between the noisy driving problem that we consider in this paper and the phonon-induced hopping in the prevailing literature.

The Einstein relation $G_{\mathrm{Ohm}} = (e/L)^2 \varrho_{\mathrm{E}} \mathcal{D}$ relates the conductance and diffusion in real space. We deduce that

$$\mathcal{D} = \left(\frac{L}{\mathcal{N}} \right)^2 [[w_{mn}^\gamma]]_{\parallel}. \quad (69)$$

This should be compared with the SLRT expression for the noise-induced energy diffusion

$$\mathcal{D}_{\mathrm{E}} = \left(\frac{1}{\varrho_{\mathrm{E}}} \right)^2 [[w_{mn}^\gamma]]_{\perp}. \quad (70)$$

Here the resistance of the network is calculated between states that reside far away in energy. The SLRT result for $\mathcal{D}_{\mathrm{E}}$ and the hopping implied result for $\mathcal{D}$ are both simple and manifestly equivalent: the diffusion coefficient equals the transition rate $\{[w_{mn}^\gamma]]$ times the *step* squared. In the SLRT calculation the step in energy space is $1/\varrho_{\mathrm{E}}$ while in the standard real-space analysis the step is $L/\mathcal{N}$. Optimization of the hopping with respect to the distance ω in energy is equivalent to optimization with respect to the distance r in space.

XI. CAN WE GET VRH FROM KUBO?

The analysis that we have introduced in this paper gives the impression that SLRT is essential in order to derive the VRH result. This statement looks to be in contradiction with the prevailing common wisdom and therefore deserves further clarification. In the discussion below we explain that VRH can be obtained from Kubo for an *artificial* toy model but not for the *physical* model that we have analyzed in this paper following Anderson and Mott.

It is instructive to point out that the Kubo formula, Eq. (39), can be rephrased as saying that

$$D = [D_n]_{\mathrm{avr}}, \quad (71)$$

where D_n is the diffusion coefficient for a spreading process that start at state n. If we consider an artificial model where

the eigenstates are labeled as $n = (i\nu)$ with energies $E_{i\nu} = \epsilon_\nu$ and matrix elements $V_{i\nu,j\mu} \sim \exp(-|r_i - r_j|/\ell_\xi)$, such that

$$w_{i\nu,j\mu} \sim \exp\left[-\frac{|r_i - r_j|}{\ell_\xi} - \frac{|\epsilon_\nu - \epsilon_\mu|}{\omega_c} \right] \quad (72)$$

then all the D_n are the same value. Furthermore, their common value is given by a VRH-like expression which reflects an optimization of the hopping distance. Consequently, the average D is also given by the exactly the same VRH-like expression.

However, in the physical model that we have considered in this paper the D_n in the Anderson regime are typically dominated by one term only and therefore wildly fluctuate. It is then clear that an algebraic average would give a very large result which is dominated by the minority of large elements. In fact our analysis, which merely reproduces Mott's original analysis, shows that up to logarithmic correction the Kubo formula gives $G \propto \omega_c^2$. In order to get VRH we have to perform an SLRT analysis rather than LRT analysis.

In the above discussion one could wonder whether a good strategy for obtaining an SLRT estimate would be to take a harmonic instead of algebraic average over D_n. In fact there are circumstances where such procedure gives a very good result.[1] However, in general, such procedure is expected to underestimate the correct result because it is based on the assumption that the hopping is always with the same optimal step, as in series addition of resistors, without the possibility to bypass in parallel.

XII. VRH VS HOPPING

It is customary to assume that a noisy nonthermal source has a Lorentzian power spectrum

$$\tilde{F}(\omega) = \frac{1}{\pi} \frac{\omega_c}{\omega^2 + \omega_c^2}. \quad (73)$$

Let us consider the Anderson regime and assume that $\omega_c \ll \Delta_\xi$. It should be clear that the VRH result is not applicable here. This is because the transport is dominated by $\omega > \Delta_\xi$ transitions. In this case SLRT give the same result as Kubo, which we call simple hopping[9]

$$\mathcal{D} \approx \omega_c t_{\mathrm{loc}} \mathcal{D}_0 = \frac{(\ell_\xi)^2}{t_c}, \quad (74)$$

where $t_c = 1/\omega_c$. This is as expected from heuristic considerations. It describes a random walk hopping process with steps of size ℓ_ξ and time τ_γ. This type of result has been highlighted in old studies of the quantum-kicked rotator problem.[24]

XIII. EXPERIMENTAL DEMONSTRATION OF SEMI LINEAR RESPONSE

For a given metallic ring the experimentalist has control over the frequency and on the strength of the driving. These can be adjusted such that FGR transitions are the dominant mechanism for energy absorption. This excludes the adiabatic regime where near-neighbor transitions dominate either

due to Landau-Zener[17] or Debye relaxation mechanism.[16]

Assuming that FGR transitions are the dominant mechanism, this does not automatically imply linear response. The rate of the driven transitions can be smaller or larger compared with the environmental induced rate of transitions and accordingly we expect a crossover from LRT to SLRT.[1]

The simple-minded indication for semilinear response is a drop in the value of the absorption coefficient if the driving is strong enough (see estimates below). What can be measured is the SLRT suppression factor g_{SLRT} and its dependence on the spectral content of the driving.

As observed in Ref. 3, the distinction of semilinear from linear response is not ambiguous. The theory is called SLRT because on the one hand the power spectrum $\widetilde{S}(\omega) \mapsto \lambda \widetilde{S}(\omega)$ leads to $D \mapsto \lambda D$ but on the other hand $\widetilde{S}(\omega) \mapsto \widetilde{S}_1(\omega) + \widetilde{S}_2(\omega)$ does not lead to $D \mapsto D_1 + D_2$. This semilinearity can be tested in an experiment in order to distinguish it from linear response.

Let us discuss in more details the experimental conditions that are required in order to observe semilinear response. The problem is characterized by the following parameters:

$$\text{system:} \quad (\omega_0, \omega_c^{sys}), \tag{75}$$

$$\text{driving:} \quad (\omega_c, \varepsilon), \tag{76}$$

$$\text{bath:} \quad (\gamma_\phi, \gamma_{rlx}), \tag{77}$$

where ω_c^{sys} is the frequency that characterizes the semiclassical motion; $\omega_0 = \varrho_E^{-1}$ is the frequency corresponding to the mean-level spacing; ω_c and ε are the cut-off frequency and the RMS value of the driving (EMF); and $\gamma_\phi, \gamma_{rlx}$ are the dephasing and the relaxation rates due to the environment.

As already stated we are not interested in adiabatic driving ($\omega_c < \omega_0$) but rather in what we call dc driving. The conditions that have to be satisfied in an SLRT-oriented experiment are

$$\text{dc driving:} \quad \omega_0 \ll \omega_c \ll \omega_c^{sys}, \tag{78}$$

$$\text{FGR condition:} \quad \omega_0 \ll w_\varepsilon \ll \omega_c, \tag{79}$$

$$\text{LRT condition:} \quad w_\varepsilon \ll \gamma, \tag{80}$$

$$\text{SLRT condition:} \quad \gamma \ll w_\varepsilon, \tag{81}$$

where w_ε is the FGR transition rate [Eq. (36)].

There are several experimental methods which could support the theoretical predictions of our paper. The experiment can be based on metallic rings (gold,[25,26] copper,[27] silver[28]), GaAs and other semiconductor heterostructures,[29,30] molecular wires, etc. To estimate the experimental numbers let us consider a semiconductor (GaAs) ring driven by time-dependent magnetic flux

$$\mathcal{M} = 5, \quad L = 0.1 \ \mu\text{m}, \quad \ell = 50 \ \mu\text{m}, \tag{82}$$

$$v_F = 2.7 \times 10^5 \ \text{m/s}. \tag{83}$$

The long mean-free path is required in order to be deep in the ballistic regime with sparsity

$$q = \mathcal{M} \frac{L}{\ell} \sim 0.01. \tag{84}$$

By Eq. (11) the mean-level spacing is

$$\omega_0 = \frac{2v_F}{\mathcal{M}L} \approx 1 \ \text{meV}. \tag{85}$$

The ballistic time is $t_L = L/v_F \approx 3.7 \times 10^{-13}$ s hence

$$\omega_c^{sys} = \frac{2\pi v_F}{L} \approx 11 \ \text{meV}, \tag{86}$$

which is $\sim 10^{13}$ Hz in frequency units. In order to satisfy the dc driving condition we assume a power spectrum of width $\omega_c \lesssim \omega_c^{sys}$. The EMF is induced by a time-dependent magnetic field $\varepsilon \approx (\omega_c L^2)B$. The FGR rate is estimated using Eq. (36) with $E_n - E_m \sim \omega_0$

$$w_\varepsilon \approx \frac{e^2 \mathcal{M}^3 L}{\omega_c \ell} \times \varepsilon^2 \approx \frac{e^2 \mathcal{M}^3 L^5 \omega_c}{\ell} \times B^2. \tag{87}$$

In order to satisfy the FGR condition the magnetic field should be at least 180G. The expected crossover between linear to semi-linear response occurs for $w_\varepsilon \sim \gamma$. Assuming, for example, $t_{rlx} \sim 2 \times 10^{-12}$ s we get $\gamma \sim 3\omega_0$ leading to

$$B_{SLRT \ threshold} \sim 320G. \tag{88}$$

Under the above conditions we expect that as B is increased there will be crossover from linear to semilinear response with suppression factor $g_{SLRT} \approx 0.3$, where we used Eq. (51). The crossover is of course not sharp because w_ε is after all distributed over a wide range. In fact the functional shape of the crossover can be used in order to deduce this distribution.[31] In any case it should be reemphasized that the experimental verification for the nature of the crossover requires merely to test whether the absorption rate depends in a nonlinear way on the spectral content of the driving.

XIV. SUMMARY AND DISCUSSION

Possibly the nicest thing about SLRT is that it consists a natural extension of LRT that places under one roof various results for the conductance in different regimes. It should be clear that in the strict dc limit ($\omega_c \to 0$), irrespective of the functional form of the power spectrum, we always get for G a result that formally agrees with the Landauer formula. See the discussion in Sec. II B. In the diffusive regime it becomes equivalent to the Drude formula with small weak localization corrections. But in the other regimes (Anderson and Ballistic), if the low-frequency driving has some arbitrary spectral content, then very different results are obtained (Hopping, VRH, and generalized VRH).

It is interesting that in our "minimal" treatment of the problem there is no need to introduce relaxation due to phonons in order to get a VRH result. Rather, we regard VRH as arising from the competition between the statistical properties of the matrix elements and the power spectrum of a noisy driving field.

The formalism allows to take various limits involving the size of the system (L), the driving frequency (ω_c) and its

intensity (ε), and the rate of the environmentally induced transitions (γ). The order of the limits is very important. In particular: if we take the limit $L \to \infty$ followed by $\varepsilon \to 0$, keeping γ constant, then we get LRT; while if we take $L \to \infty$ followed by $\gamma \to 0$, keeping ε constant, then we get SLRT. Also note that if we keep L constant and take $\omega_c \to 0$ we get the adiabatic limit and not the dc limit of LRT/SLRT.

We have dedicated Sec. XIII to introduce actual estimates that are required in order to observe SLRT in a real experiment. It is important to realize that the experimental procedure allows to distinguish in a nonambiguous way between LRT and SLRT by playing with the spectral content of the driving source. Furthermore, one can test specific predictions for the g_{SLRT} suppression factor, e.g., Eq. (50) with Eq. (67), and Eq. (51) with Eq. (59) or Eq. (61). We note that the explicit incorporation of the environmentally induced transitions into the resistor-network calculation and the subsequent analysis of the resulting SLRT steady state is straightforward.[31]

The SLRT calculation is based on a resistor network picture of transitions between energy levels, for which an RMT framework is very appropriate and effective. In the so called "quantum chaos" context Wigner (in the nuclear context) and later Bohigas (in the mesoscopic context) have motivated the interest in Gaussian ensembles but there are circumstances where non-Gaussian ensembles are appropriate, which lead to novel physics. Indeed we have faced in this paper the analysis of log-normal and log-box ensembles corresponding to the weak and strong disorder limits. We have demonstrated that for such ensembles a large SLRT suppression effect is expected that could not be anticipated within the LRT framework.

APPENDIX A: THE RESISTOR NETWORK CALCULATION

In this appendix we explain how the inverse resistivity $G = [[G_{nm}]]$ of a one-dimensional resistor network is calculated. We use the language of electrical engineering for this purpose. In general this relation is semilinear rather than linear, namely, $[[\lambda G]] = \lambda[[G]]$, but $[[A+B]] \neq [[A]] + [[B]]$. The experimental implications of this observation in the SLRT context are discussed in Sec. XIII.

There are a few cases where an analytical expression is available. If only near-neighbor nodes are connected, allowing $G_{n,n+1} = g_n$ to be different from each other, then "addition in series" implies that the inverse resistivity calculated for a chain of length N is

$$G = \left[\frac{1}{N} \sum_{n=1}^{N} \frac{1}{g_n} \right]^{-1}. \tag{A1}$$

If $G_{nm} = g_{n-m}$ is a function of the distance between the nodes n and m then it is a nice exercise to prove that "addition in parallel" implies

$$G = \sum_{r=1}^{\infty} r^2 g_r. \tag{A2}$$

In general an analytical formula for G is not available and we have to apply a numerical procedure. For this purpose we imagine that each node n is connected to a current source I_n. The Kirchhoff equations for the voltages are

$$\sum_m G_{mn}(V_n - V_m) = I_n. \tag{A3}$$

This set of equation can be written in a matrix form

$$\boldsymbol{GV} = \boldsymbol{I}, \tag{A4}$$

where the so-called discrete Laplacian matrix of the network is defined as

$$\boldsymbol{G}_{nm} = \left[\sum_{n'} G_{n'n} \right] \delta_{n,m} - G_{nm}. \tag{A5}$$

This matrix has an eigenvalue zero which is associated with a uniform voltage eigenvector. Therefore, it has a pseudoinverse rather than an inverse and the Kirchhoff equation has a solution if and only if $\Sigma_n I_n = 0$. In order to find the resistance between nodes $n_{in} = 0$ and $n_{our} = N$, we set $I_0 = 1$ and $I_N = -1$ and $I_n = 0$ otherwise, and solve for V_0 and V_N. The inverse resistivity is $G = [(V_0 - V_N)/N]^{-1}$.

APPENDIX B: MODEL DETAILS

In the numerical study we consider the Anderson tight binding model, where the lattice is of size $L \times M$ with $M \ll L$, and lattice constant a. The longitudinal and the transverse hopping amplitudes per unit time are $c_\parallel$ and $c_\perp$, respectively. The random on-site potential in the Anderson tight-binding model is given by a box distribution of width determined by W.

The numerical calculations of Ref. 12 assume $c_\parallel = 1$ and $c_\perp = 0.9$. Thus in the middle of the band there is a finite-energy window with exactly $\mathcal{M} = M$ open modes. Rings of length $L = 500$ with $M = 10$ modes has been considered. In our reprocessed Fig. 2 the default cutoff is $\varrho_E \omega_c \approx 7$ as in Ref. 12 but as the disorder becomes weaker it is adjusted such that the dc condition $\varrho_E \omega_c \lesssim b$ is always satisfied.

For white (uncorrelated) disorder the Hamiltonian is given by Eq. (9) with the isotropic scattering term

$$|U_{\boldsymbol{nm}}|^2 \approx \frac{a}{\mathcal{M}L} W^2. \tag{B1}$$

The eigenstates of the Hamiltonian can be found numerically. The degree of ergodicity is characterized by the participation number $PN \equiv [\Sigma \rho^2]^{-1}$, which is calculated in various representations: in position space $\rho_{r_x,r_y} = |\langle r_x, r_y | \Psi \rangle|^2$, in position-mode space $\rho_{r_x,k_y} = |\langle r_x, k_y | \Psi \rangle|^2$, and in mode space $\rho_{k_y} = \Sigma_{r_x} |\langle r_x, k_y | \Psi \rangle|^2$, where $k_y = [\pi/(\mathcal{M}+1)] \times$ integer.

APPENDIX C: THE DRUDE FORMULA

The velocity-velocity correlation function, assuming isotropic scattering, is proportional to the survival probability

$P(t) = e^{-t/t_\ell}$. Ignoring a factor that has to do with the dimensionality $d = 2, 3$ of the sample the relation is

$$\langle v(t)v(0) \rangle \approx v_E^2 P(t) = v_E^2 e^{-|t|/t_\ell}. \quad (C1)$$

The rate of the scattering can be calculated from the FGR, also know as the Born approximation

$$\frac{1}{t_\ell} = 2\pi \varrho_E |U_{mn}|^2 = \frac{\pi a}{v_E} W^2, \quad (C2)$$

where in the last equality we used Eq. (B1). From here we deduce that the mean-free path (disregarding prefactors of order unity)

$$\ell = v_E t_\ell \approx \frac{1}{a} \left(\frac{v_E}{W} \right)^2 \quad (C3)$$

and the diffusion coefficient in real space

$$\mathcal{D}_0 = \frac{1}{2} \int_{-\infty}^{\infty} \langle v(t)v(0) \rangle \approx v_E \ell. \quad (C4)$$

By the Einstein relation we deduce the Drude formula

$$G_{Ohm} = \left(\frac{e}{L} \right)^2 \varrho_E \mathcal{D}_0 = \frac{e^2}{2\pi\hbar} \mathcal{M} \frac{\ell}{L}. \quad (C5)$$

A literally equivalent route to derive the Drude formula is to semiclassically deduce $\langle\langle |v_{mn}|^2 \rangle\rangle$ from the velocity-velocity correlation function as in Sec. VII and then to substitute in Eq. (19). This has the advantage of allowing easy generalizations of the Drude formula in the ballistic and in the Anderson regimes. In this context it is useful to realize[32] that in the semiclassical picture the integral over the velocity-velocity correlation function is related to the transmission g_0 of the ring (if it were dissected). This leads to the identification in Eq. (24).

In the diffusive regime Mott has demonstrated that it is optionally possible to obtain a direct estimate of the dipole matrix elements, using a random-wave picture. Namely, it is assumed that in the diffusive regime the eigenstates of the Hamiltonian are ergodic in position space and look like random waves with a correlation scale ℓ. Locally the eigenstates are similar to free waves. The total volume L^d is divided into domains of size ℓ^d. Hence we have $(L/\ell)^d$ such domains. Given a domain, the condition to have nonvanishing overlap upon integration is $|\vec{q}_n - \vec{q}_m|\ell < 2\pi$, where $\vec{q}$ is the local wave number within this domain. The probability that $\vec{q}_n$ would coincide with $\vec{q}_m$ is $1/(k_E\ell)^{d-1}$. The contributions of the non-zero overlaps add with random signs hence

$$|v_{mn}| = \left[\frac{1}{(k_E\ell)^{d-1}} \times \left(\frac{L}{\ell} \right)^d \right]^{1/2} \times (\overline{\Psi^2}\ell^d) v_E. \quad (C6)$$

Assuming ergodicity $\overline{\Psi^2} \approx 1/L^d$ and we get the same estimate as in the semiclassical procedure.

APPENDIX D: THE LOG-BOX ENSEMBLE

The cumulative distribution function that corresponds to Eq. (28) is

$$\text{Prob}(X < x) = \frac{\ln x - \ln x_0}{\ln(x_1/x_0)}. \quad (D1)$$

The algebraic, geometric, and harmonic averages are

$$\langle\langle x \rangle\rangle_a = \frac{x_1 - x_0}{\ln(x_1/x_0)}, \quad (D2)$$

$$\langle\langle x \rangle\rangle_g = \sqrt{x_1 x_0}, \quad (D3)$$

$$\langle\langle x \rangle\rangle_h = \ln(x_1/x_0) \frac{x_1 x_0}{x_1 - x_0}. \quad (D4)$$

Note that for this distribution the median equals the geometric average. The sparsity parameters are

$$s = 2\tilde{p} \frac{e^{-1/\tilde{p}} - 1}{e^{-1/\tilde{p}} + 1}, \quad (D5)$$

$$p = -\tilde{p}[\ln \tilde{p} + \ln(1 - e^{-1/\tilde{p}})], \quad (D6)$$

$$q = \left(2\tilde{p} \sinh \frac{1}{2\tilde{p}} \right)^{-1}, \quad (D7)$$

where we defined $\tilde{p} = (\ln(x_1/x_0))^{-1}$. If the distribution is very stretched reasonable approximations are

$$s \approx 2\tilde{p}, \quad (D8)$$

$$p \approx -\tilde{p} \ln \tilde{p}. \quad (D9)$$

For the VRH calculation

$$x_\omega = x_1 \left(\frac{x_0}{x_1} \right)^{1/\varrho_E\omega} \approx \frac{\langle\langle x \rangle\rangle_a}{\tilde{p}} \exp\left(-\frac{1}{\tilde{p}\varrho_E\omega} \right). \quad (D10)$$

For a rectangular $\tilde{F}(\omega)$ the VRH optimization is trivial and gives $\omega \approx x_{\omega_c}$, leading to

$$g_{SLRT} \approx \frac{1}{\tilde{p}} \exp\left[-\frac{1}{\tilde{p}\varrho_E\omega_c} \right]. \quad (D11)$$

For an exponential $\tilde{F}(\omega)$ the VRH optimization gives

$$g_{SLRT} \approx \frac{1}{\tilde{p}} \exp\left[-2\left(\frac{1}{\tilde{p}\varrho_E\omega_c} \right)^{1/2} \right], \quad (D12)$$

which is the same as in the traditional VRH optimization.

APPENDIX E: THE LOG-NORMAL ENSEMBLE

The cumulative distribution function that corresponds to Eq. (29) is

$$\text{Prob}(X < x) = \frac{1}{2} + \frac{1}{2} \text{erf}\left[\frac{\ln(x) - \mu}{\sigma\sqrt{2}} \right]. \quad (E1)$$

The algebraic, geometric, and harmonic averages are

$$\langle\langle x \rangle\rangle_a = e^{\mu + \sigma^2/2}, \quad (E2)$$

$$\langle\langle x \rangle\rangle_{\mathrm g} = e^{\mu}, \qquad (\mathrm{E3})$$

$$\langle\langle x \rangle\rangle_{\mathrm h} = e^{\mu - \sigma^2/2}. \qquad (\mathrm{E4})$$

The sparsity parameters are

$$s = q^2, \qquad (\mathrm{E5})$$

$$p = \frac{1}{2}\mathrm{erfc}\left(\frac{\sigma}{2\sqrt{2}}\right), \qquad (\mathrm{E6})$$

$$q = e^{-\sigma^2/2}. \qquad (\mathrm{E7})$$

The VRH estimate is

$$x_{\omega} = \exp\left[\mu + \sigma\sqrt{2}\,\mathrm{erfinv}\left(1 - \frac{2}{\varrho_{\mathrm E}\omega}\right)\right]$$

$$\approx \langle\langle x \rangle\rangle_{\mathrm g} \exp\left[\sqrt{\ln\left(\frac{1}{q}\right)^2\left(\ln\frac{\varrho_{\mathrm E}^2\omega^2}{2\pi} - \ln\ln\frac{\varrho_{\mathrm E}^2\omega^2}{2\pi}\right)}\right].$$

$$(\mathrm{E8})$$

For a rectangular $\widetilde{F}(\omega)$ the VRH optimization is trivial and gives $\omega \approx x_{\omega_c}$, leading to

$$g_{\mathrm{SLRT}} \approx q\,\exp[2\sqrt{-\ln q\,\ln(\varrho_{\mathrm E}\omega_c)}]. \qquad (\mathrm{E9})$$

For an exponential $\widetilde{F}(\omega)$ the VRH optimization gives

$$g_{\mathrm{SLRT}} \approx q\,\exp\left[\sqrt{-\ln q\,\ln\frac{-\varrho_{\mathrm E}^2\omega_c^2\ln q}{\pi}} - \sqrt{\frac{\sqrt{-4\pi\ln q}}{\varrho_{\mathrm E}\omega_c}}\right]$$

$$\approx q\,\exp[\sqrt{-2\ln q\,\ln(\varrho_{\mathrm E}\omega_c)}]. \qquad (\mathrm{E10})$$

Due to the minority dominance the functional form is more robust compared with the log-box case.

---

[1] D. Cohen, T. Kottos, and H. Schanz, J. Phys. A **39**, 11755 (2006).

[2] S. Bandopadhyay, Y. Etzioni, and D. Cohen, Europhys. Lett. **76**, 739 (2006).

[3] M. Wilkinson, B. Mehlig, and D. Cohen, Europhys. Lett. **75**, 709 (2006).

[4] N. F. Mott, Philos. Mag. **22**, 7 (1970); N. F. Mott and E. A. Davis, *Electronic Processes in Non-Crystalline Materials*, (Clarendon Press, Oxford, 1971).

[5] A. Miller and E. Abrahams, Phys. Rev. **120**, 745 (1960).

[6] V. Ambegaokar, B. Halperin, and J. S. Langer, Phys. Rev. B **4**, 2612 (1971).

[7] M. Pollak, J. Non-Cryst. Solids **11**, 1 (1972).

[8] B. I. Shklovskii and A. L. Efros, *Electronic Properties of Doped Semiconductors* (Springer-Verlag, Berlin, 1984).

[9] D. Cohen, Phys. Rev. B **75**, 125316 (2007).

[10] E. Wigner, Ann. Math **62**, 548 (1955); **65**, 203 (1957).

[11] O. Bohigas, in *Chaos and Quantum Physics*, Proceedings of the Les-Houches Summer School, Session LII, edited by A. Voros and M.-J. Giannoni (North-Holland, Amsterdam, 1990).

[12] A. Stotland, R. Budoyo, T. Peer, T. Kottos and D. Cohen, J. Phys. A **41**, 262001 (2008).

[13] A. Stotland, D. Cohen, and N. Davidson, EPL **86**, 10004 (2009).

[14] For deviation from Gaussian distributions see: T. Prosen and M. Robnik, J. Phys. A **26**, L319 (1993); E. J. Austin and M. Wilkinson, Europhys. Lett. **20**, 589 (1992); Y. Alhassid and R. D. Levine, Phys. Rev. Lett. **57**, 2879 (1986).

[15] Y. V. Fyodorov, O. A. Chubykalo, F. M. Izrailev, and G. Casati, Phys. Rev. Lett. **76**, 1603 (1996).

[16] The first studies have addressed mainly the Debye regime: M. Büttiker, Y. Imry, and R. Landauer, Phys. Lett. **96A**, 365 (1983); R. Landauer and M. Büttiker, Phys. Rev. Lett. **54**, 2049 (1985); M. Büttiker, Phys. Rev. B **32**, 1846 (1985); Ann. N.Y. Acad. Sci. **480**, 194 (1986).

[17] In the deep adiabatic regime the Landau-Zener mechanism might be of relevance: M. Wilkinson, J. Phys. A **21**, 4021 (1988).

[18] The Kubo formula is applied to diffusive rings in: Y. Imry and N. S. Shiren, Phys. Rev. B **33**, 7992 (1986); N. Trivedi and D. A. Browne, *ibid.* **38**, 9581 (1988).

[19] Weak-localization corrections were studied in: B. Reulet and H. Bouchiat, Phys. Rev. B **50**, 2259 (1994); A. Kamenev, B. Reulet, H. Bouchiat, and Y. Gefen, Europhys. Lett. **28**, 391 (1994).

[20] For a review see A. Kamenev and Y. Gefen, Int. J. Mod. Phys. B **9**, 751 (1995).

[21] Measurements of conductance of closed diffusive rings are described by: B. Reulet, M. Ramin, H. Bouchiat, and D. Mailly, Phys. Rev. Lett. **75**, 124 (1995).

[22] Measurements of susceptibility of individual closed rings using SQUID is described in: N. C. Koshnick, H. Bluhm, M. E. Huber, and K. A. Moler, Science **318**, 1440 (2007).

[23] A new micromechanical cantilevers technique for measuring currents in normal metal rings is described in: A. Bleszynski-Jayich, W. Shanks, R. Ilic, and J. Harris, J. Vac. Sci. Technol. B **26**, 1412 (2008).

[24] E. Ott, T. M. Antonsen, Jr., and J. D. Hanson, Phys. Rev. Lett. **53**, 2187 (1984); D. Cohen, Phys. Rev. A **44**, 2292 (1991).

[25] E. M. Q. Jariwala, P. Mohanty, M. B. Ketchen, and R. A. Webb, Phys. Rev. Lett. **86**, 1594 (2001).

[26] H. Bluhm, N. C. Koshnick, J. A. Bert, M. E. Huber, and K. A. Moler, Phys. Rev. Lett. **102**, 136802 (2009).

[27] L. P. Lévy, G. Dolan, J. Dunsmuir, and H. Bouchiat, Phys. Rev. Lett. **64**, 2074 (1990).

[28] R. Deblock, R. Bel, B. Reulet, H. Bouchiat, and D. Mailly, Phys. Rev. Lett. **89**, 206803 (2002).

[29] D. Mailly, C. Chapelier, and A. Benoit, Phys. Rev. Lett. **70**, 2020 (1993).

[30] B. C. Lee, O. Voskoboynikov, and C. P. Lee, Physica E **24**, 87 (2004).

[31] D. Hurowitz and D. Cohen (unpublished).

[32] D. Cohen and Y. Etzioni, J. Phys. A **38**, 9699 (2005).